ARMY RESEARCH LABORATORY

Developing a Transient Finite Element Model to Simulate the Launch Environment of the 155-mm SADARM Projectile

by Stephen Wilkerson, David Hopkins, George Gazonas, and Morris Berman

ARL-TR-2341 September 2000

Approved for public release; distribution is unlimited.

Army Research Laboratory
Aberdeen Proving Ground, MD 21005-5066

ARL-TR-2341 **September 2000**

Developing a Transient Finite Element Model to Simulate the Launch Environment of the 155-mm SADARM Projectile

Stephen Wilkerson, David Hopkins, George Gazonas, and Morris Berman
Weapons and Materials Research Directorate, ARL

Abstract

Projectiles like SADARM, with delicate electronic components, need robust designs that are able to survive high "g" accelerations and spin rates. Unfortunately, the packaging of these components and their space requirements reduce the design's safety margin. Therefore, considerable care must be used in analyzing the structural package. Conventional projectiles are typically analyzed using a quasi-static, axisymmetric, finite-element approach that balances the peak propellant pressure on the base of the projectile with an equivalent acceleration. In most circumstances, the robustness of the design makes this approach more than sufficient for identifying problem areas in the structure. However, the internal components used in SADARM are sensitive to off-axis loading such as that caused by spin rate or the rapid unloading of the projectile's base that occurs at muzzle exit. Additionally, stress waves caused by balloting and impedance mismatching within the stack design only serve to further reduce the design margin. To compensate for the reduced design margin and the increased source of potentially damaging loads, more sophisticated finite-element techniques need to be employed. The techniques presented here represent a modern approach to analyzing the projectile's launch loading conditions over traditional techniques.

Table of Contents

		Page
	List of Figures	v
1.	Introduction	1
2.	Background	2
3.	Quasi-Static Analysis	3
4.	Stack Model Details	13
5.	Results	20
6.	Conclusions	24
	Distribution List	27
	Report Documentation Page	29

INTENTIONALLY LEFT BLANK.

List of Figures

Figure		Page
1.	SADARM Functionality	2
2.	SADARM Projectile	4
3.	SADARM Internal Components From a Single Munition	4
4.	Natural Frequency as a Function of Forcing Frequency	7
5.	Natural Frequency vs. Forcing Function Amplification Plot	8
6.	Crude Cylinder Model	9
7.	Refined Cylinder Model	10
8.	Results From Cylinder Models	11
9.	Comparison Between a Crude and Refined Model in DYNA3D	12
10.	Gun-Tube Finite-Element Model and Gun-Projectile Interface	14
11.	Pressure Time Curves Applied to the Base of the Projectile in the DYNA3D Finite-Element Model	15
12.	Base Pressure and Frictional Force Applied to the Projectile	15
13.	Base to Shell Attachment	16
14.	Finite-Element Model of Fuse Parts	17
15.	Finite-Element Model of SADARM's Stack Components	17
16.	Sliding Interfaces Between Stack Components in the SADARM Finite-Element Model	18
17.	Bellville Spring Interface to Simulate Compressive Load on Stack Model	19
18.	Cut-Away View of the SADARM Stack Model	19
19.	Displacement and Velocity Comparisons Between the IBHVG2 Code and DYNA3D's Finite-Element Calculations	21

Figure Page

20. Checking the Projectile's Number of Revolutions While In-Bore 21

21. Von-Mises Stress Contours at Peak Pressure for a 7R Firing.................................... 22

22. Von-Mises Stress Contours at Peak Pressure for an 8S Firing.................................. 22

23. Von-Mises Stress Contours at Peak Pressure for a 7R Firing.................................... 23

24. Von-Mises Stress Contours at Peak Pressure for an 8S Firing.................................. 23

1. Introduction

The 155-mm sense-and-destroy armor missile (SADARM) projectile is the U.S. Army's first fire-and-forget autonomous bullet and, as such, offers a significant improvement over conventional projectiles. The projectile was engineered to enable enemy engagement without a clear line of sight (LOS) while achieving a high probability of kill (P_k). Conventional 155-mm munitions are also fired at enemy positions without a clear LOS. However, conventional projectiles need to be fired in large numbers to achieve a reasonable probability of hit (P_h). The SADARM projectile represents a significant improvement over this approach due to its onboard target acquisition system. Once over the target area and at a predetermined altitude, SADARM dispenses two submunitions. Each of the submunitions is slowed in velocity and spin by parachutes while internal logic components identify, target, and attack enemy positions. This concept results in a higher P_k with a reduced number of projectiles. It also helps mitigate the probability of return fire.

Projectiles like SADARM, with delicate electronic components, need robust designs that are able to survive high "g" accelerations and spin rates. Unfortunately, the packaging of these components and their space requirements reduce the design's safety margin. Therefore, considerable care must be used in analyzing the structural package. Conventional projectiles are typically analyzed using a quasi-static, axisymmetric, finite-element approach that balances the peak propellant pressure on the base of the projectile with an equivalent acceleration. In most circumstances, the robustness of the design makes this approach more than sufficient for identifying problem areas in the structure. However, the internal components used in SADARM are sensitive to off-axis loading such as that caused by spin rate or the rapid unloading of the projectile's base that occurs at muzzle exit. Additionally, stress waves caused by balloting and impedance mismatching within the stack design only serve to further reduce the design margin. To compensate for the reduced design margin and the increased source of potentially damaging loads, more sophisticated finite-element techniques need to be employed. The techniques presented here represent a modern approach to analyzing the projectile's launch loading conditions over traditional techniques.

2. Background

As with any 155-mm projectile, there are numerous design criteria. For example, projectile attributes enabling it to be stored in varying environments for years before use, as well as the projectile's ability to survive temperature extremes and different launch pressures, are only a few of the problems facing the bullet's designers. One of the most damaging attributes of a 155-mm projectile is its launch and flight. Before describing the structural analysis that was performed on the package, a brief description of the sense-and-destroy armor missile (SADARM) functionality and its components is given. Figure 1 shows the launch, flight, submunitions expulsion, spin down, and targeting of enemy armor.

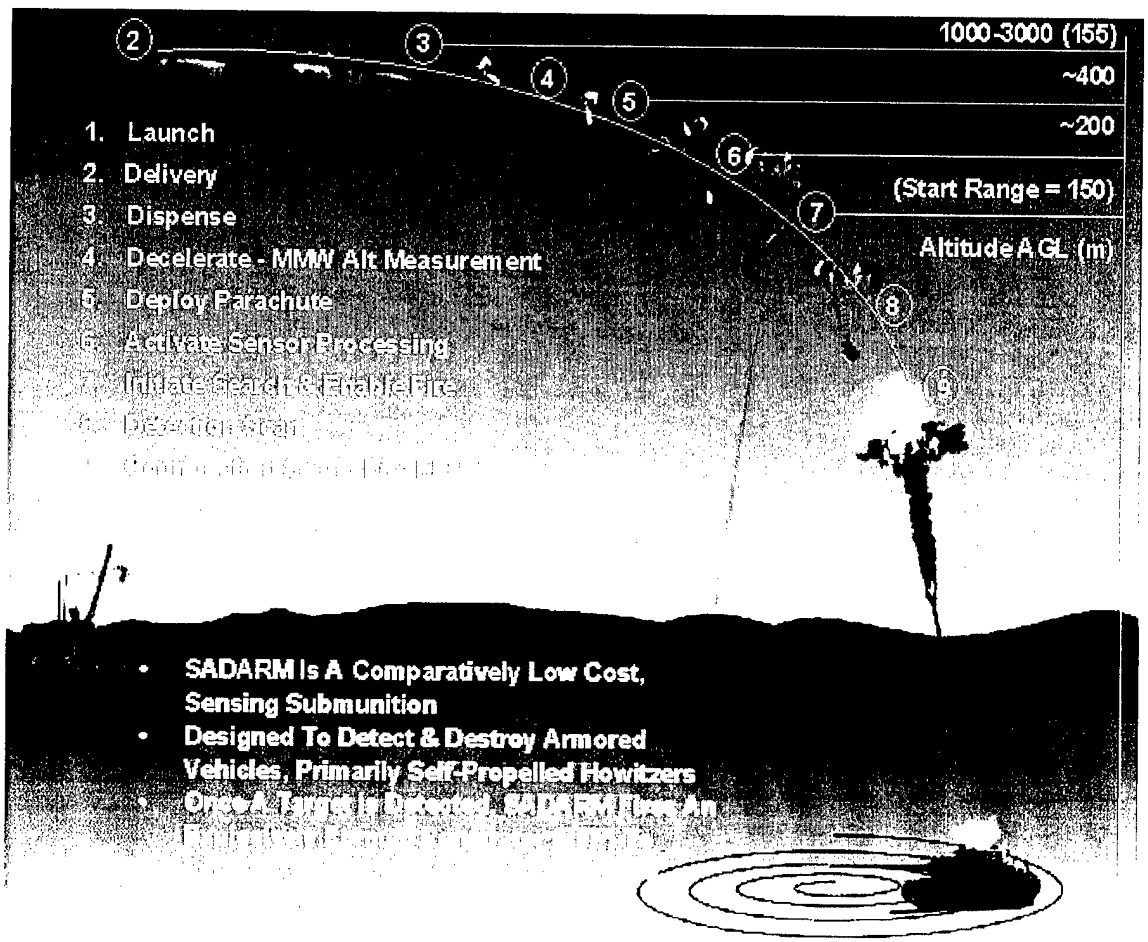

Figure 1. SADARM Functionality.

From Figure 1, during the launch (1) the SADARM projectile must survive pressure loading ranging from Zone-7R to Zone-8S. A Zone-7R firing uses a M199 propellant that accelerates the projectile to a velocity of approximately 690 m/s in about 22 ms. A Zone-8S charge firing uses a M203 propellant to accelerates the projectile to a velocity of approximately 830 m/s in just under 14 ms. Additionally, for design purposes, the projectile must be able to operate at the permissible individual maximum pressure (PIMP), plus 3 standard deviations above that pressure. This is commonly referred to as the PIMP +3 condition. During the projectile delivery, delicate electronic components are subjected to 15,000 g's acceleration and high spin rates. Therefore, it is imperative to have tools during the design process to examine the structural response of the internal and external SADARM components prior to testing. The delivery (2) of the SADARM submunitions begins prior to reaching the target and above the target area at a predetermined altitude. At that time, a small charge dispenses (3) the submunitions, which are decelerated (4). After the submunitions are decelerated by drag devices, a parachute deploys (5) and the electronic components begin searching the area below for targets using onboard active sensor processing (6), which initiates search and enables firing (7). Once the scan detects a target (8), a confirmation pass (9) is made and the target is engaged.

The SADARM projectile (Figure 2) consists of a base unit, shell casing, fuse, split pusher plate, spring, and two lethal mechanisms. The lethal mechanism assembly is shown in Figure 3 for reference. At the heart of the lethal mechanism is the electronics module assembly (EMA). The components in the EMA must be robust enough to survive the launch, flight, and expulsion events at a variety of temperatures to complete SADARM's mission.

3. Quasi-Static Analysis

The stresses during a projectile can be analyzed using a quasi-static analysis that balances the peak acceleration with the peak pressure condition. The rational behind this approach takes advantage of the fact that the pressure loading is smooth and at a low frequency. Therefore, the projectiles internal components, which may have high natural frequencies, will have insufficient

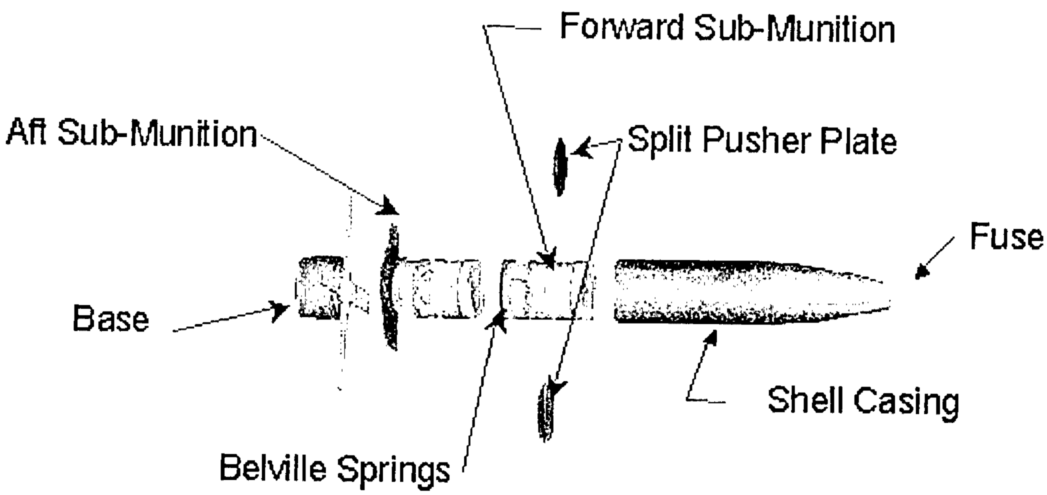

Figure 2. SADARM Projectile.

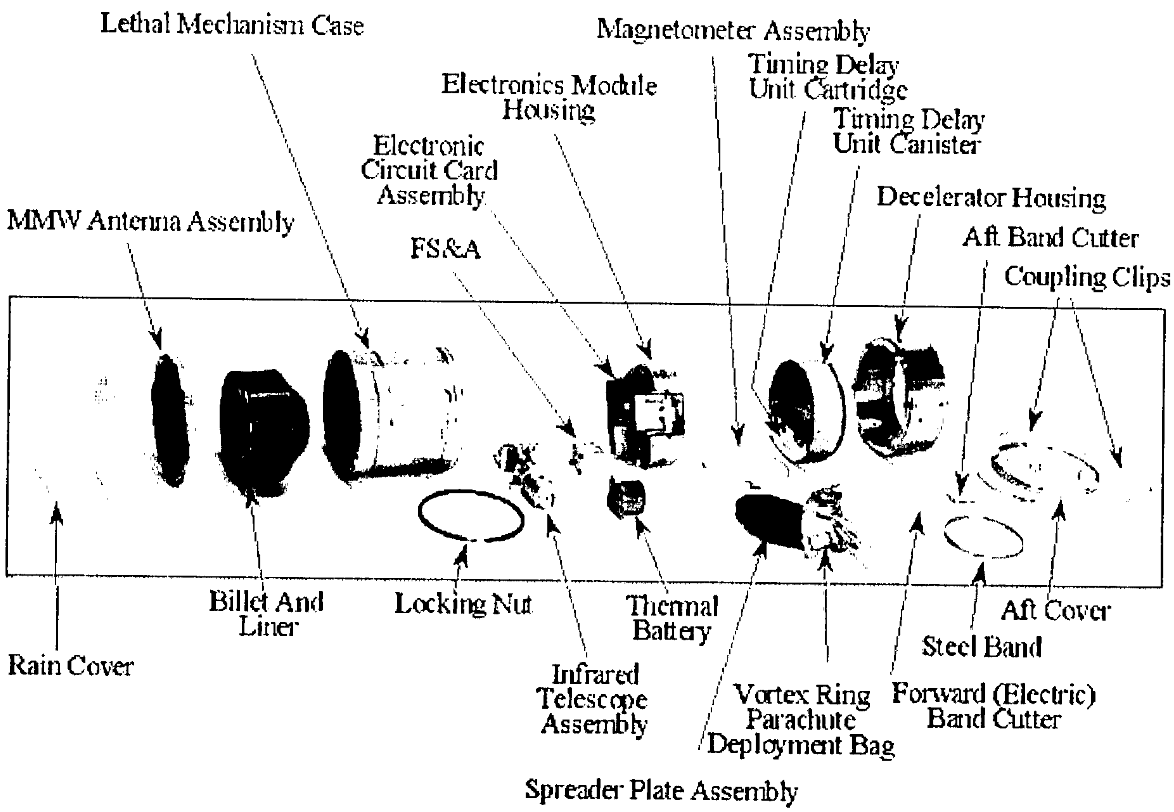

Figure 3. SADARM Internal Components From a Single Munition.

time to respond to the low-frequency input and therefore respond in a static nature. This approach has been used for years with good success and ignores transient waves, material and mechanical interfaces, and gaps. When the design margin is high, this approach presents no problem. However, the SADARM projectile is far from axisymmetric, as can be seen in Figure 3, and the design margin is not high. Therefore, additional considerations need to be taken into account. A simplistic examination of the transient portion of the loading is examined here using a spring mass system. If a one-degree of freedom system is considered, the contribution of the transient portion of the loading during launch can be estimated. Using a force balance, the basic differential equation for a spring mass under a sinusoidal loading function can be written as

$$\ddot{x} + p^2 x = q \sin(wt), \tag{1}$$

where

$$p = \sqrt{\frac{k}{m}} \text{ and } q = \frac{f}{m}. \tag{2}$$

The particular solution to the top equation can be written as

$$x = \frac{q \sin(wt)}{p^2 - w^2}. \tag{3}$$

Adding the particular solution to the general solution yields

$$x = C_1 \cos(pt) + C_2 \sin(pt) + \frac{q \sin(wt)}{p^2 - w^2}. \tag{4}$$

The first two terms of this equation represent the free vibration of the system that is dependent on the stiffness (k) and the mass (m), and the last term is due to the forced vibration of the system and its frequency $(w)/2\pi$. For the transient case,

$$C_1 = x_0 \text{ and } C_2 = \frac{x_0}{p} - \frac{\frac{qw}{p}}{p^2 - w^2}. \tag{5}$$

If a launch-type environment is considered, initial conditions are zero initial displacement and velocity $x_0 = 0$ and $\dot{x}_0 = 0$. The solution to the displacement field can then be written as

$$x = \frac{q}{p^2 - w^2}\left[\sin(wt) - \frac{w}{p}\sin(pt)\right]. \tag{6}$$

Examining this equation, the free vibration contribution and the forced vibration portions can be easily identified. To simplify this equation, a half-sin pulse is applied as the loading function, letting $w = \pi$ and varying the time $0 < t < 1$. Now, the natural frequency of the system is allowed to vary as a function of the forcing function, $p = (\%)w$. Finally, normalizing the loading, $q = \frac{f}{m} = 1.0$. By doing this, the influence of the transient component of the displacement can be seen as a function of the frequency difference between the forcing function and the natural frequency of the system. A table examining the contribution of the natural frequency of the system vs. the forcing function frequency is given in Figure 4. Letting the natural frequency (p) = 1.1, 2, 5, 11, 21, 31, 51, and 100 times the forcing function frequency (w) shows the dynamic amplification caused when the natural frequency is close to the forcing function frequency. Figures 4 (a) and 4 (b), where p = *1.1* and *2.0* w, respectively, show dynamic amplification. However, as p becomes larger than w, contribution from the structures natural frequency becomes negligible and completely disappears when $p >> w$. A three-dimensional (3-D) representation with *1.1* $w < p$ *20* w is provided in Figure 5.

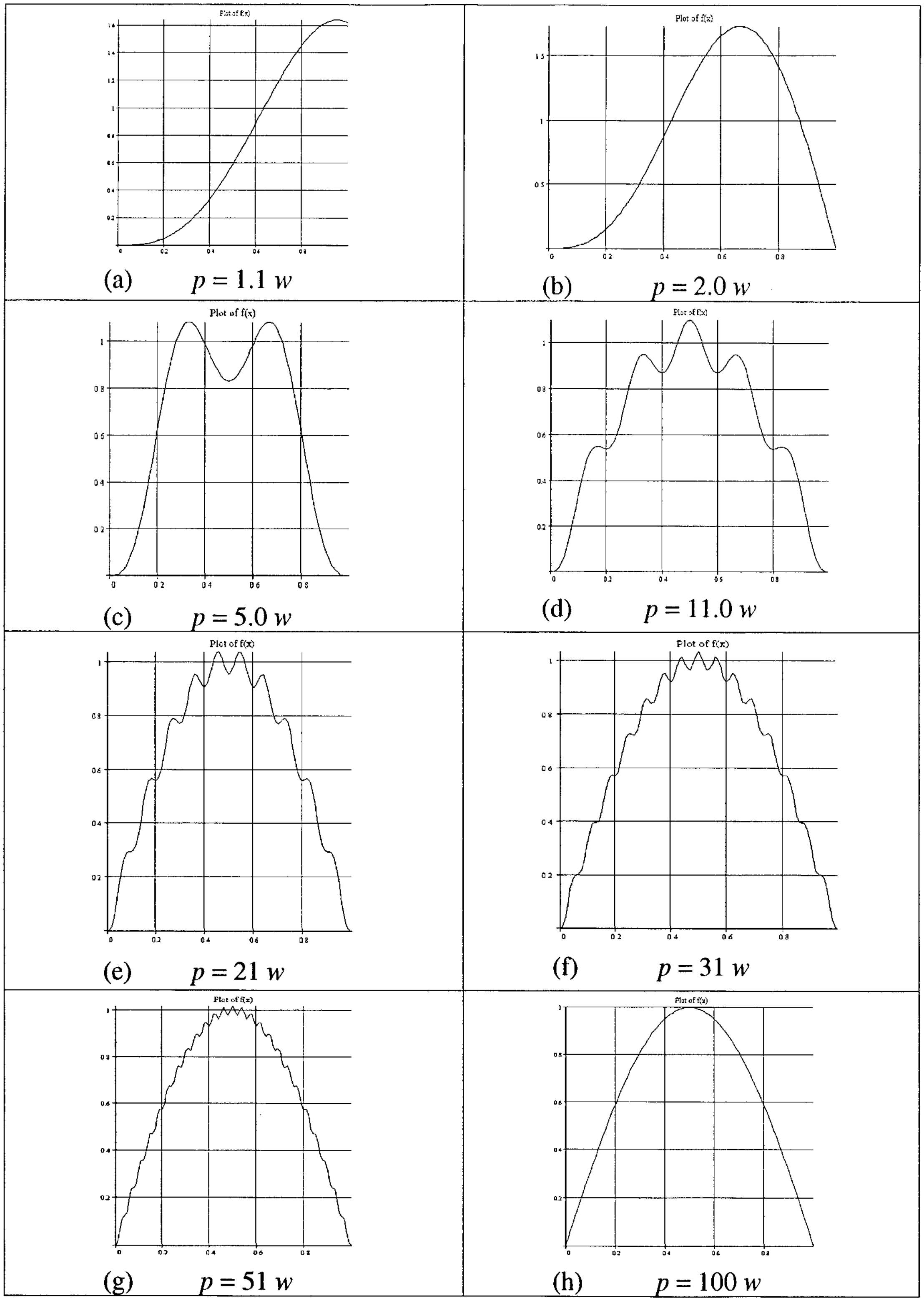

Figure 4. Natural Frequency as a Function of Forcing Frequency.

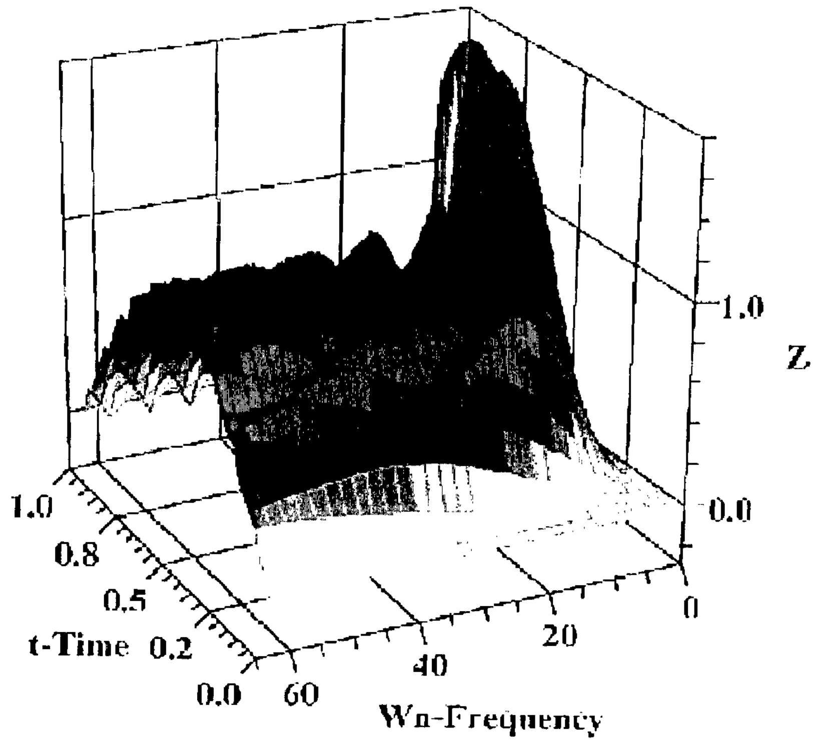

Figure 5. Natural Frequency vs. Forcing Function Amplification Plot.

In Figure 5, W_n frequency is p absolute. So, $W_n = 60$ is approximately $p \cong 20\ w \cong 20\ \pi$. Of particular interest is whether the transient component needs to be considered when examining the SADARM projectile. The SADARM projectile launch time is approximately 14 ms, which equates to a frequency of approximately 70 Hz. On the other hand, if the axial frequency of the shell casing is considered, it may be found that this frequency is much higher. The projectile's shell casing is made of steel and is approximately 30 in long. Recognizing that the wave speed is $\sqrt{E/\rho}$, it is found that the speed of sound in steel is approximately 200,000 in/s. Therefore, the wave propagation time from one end to the other and the relaxation wave's return time will be related to the first axial mode of the projectile. The frequency will be approximately 3,400 Hz. This would be approximately 50× the forcing frequency for the SADARM projectile. Therefore, it is safe to assume the quasi-static loading state when examining the stresses at peak pressure for most cases. While this is a perfectly safe assumption for designing the shell base and casing, this may not be the limiting design feature for this projectile's internal components.

Spin and shot exit and expulsion also cause stresses in the projectile and subcomponents. As a check of the shot-exit condition, a simplistic model is examined using the DYNA3D transient code. This analysis is discussed briefly to highlight the importance of stress waves that may exist due to the rapid unloading of the projectile at muzzle exit. For this problem, two models were constructed, one with a course grid and another with a finer grid representation. Figures 6 and 7 show the course- and fine-grid representation of a 30-in cylinder. The back end of both cylinders is pressurized with a normalized pressure-time curve similar to the one used to launch the SADARM projectile.

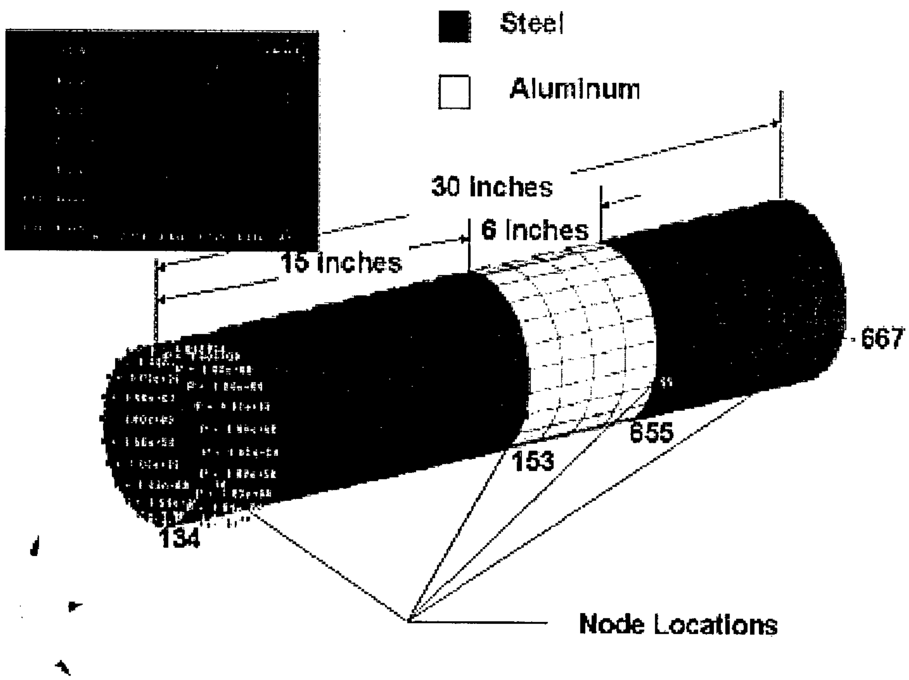

Figure 6. Crude Cylinder Model.

The cylinder also has a material change at its midsection. In the red sections, the modulus and density is that of steel. However, the modulus is changed to aluminum in the yellow section. This was done to examine whether or not possible impedance mismatching would result in reflection waves possibly elevating the stress level in internal components within the SADARM stack model. The results are briefly discussed here as part of the argument in favor of a transient

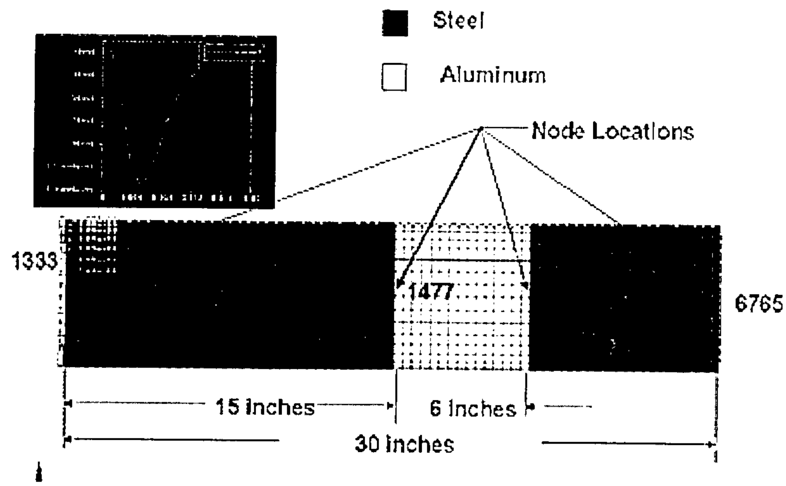

Figure 7. Refined Cylinder Model.

analysis. The SADARM projectile consists of a dozen or more free-surface interfaces, gaps, and huge impedance mismatches within the stack model. Therefore, it is critical to ascertain whether or not these structural attributes are important enough to be considered in the model. Equally important is that all of these would-be stress risers are completely ignored by a quasi-static implicit analysis of the structure.

The results from these two analyses are presented in Figure 8 for the nodes highlighted. The plots examine the axial nodal acceleration. Two important features are very evident from this analysis. The first is that there is considerable high-frequency ringing within the cylinder at shot exit. This high-frequency component may or may not be near-resonant frequencies of SADARM's internal electronic components, a point that is returned to later. The second notable feature is the difference of the response at the material interfaces. This can clearly be seen when comparing the response at shot exit at node 153 and 667 in the crude model and nodes 1477 and 6765 in the refined model. As can be seen, in some cases, the stress amplification is attenuated and, in others, it is amplified. This simple example demonstrates the possible importance of impedance mismatching and free interfaces. As a final check of the two models, a comparison

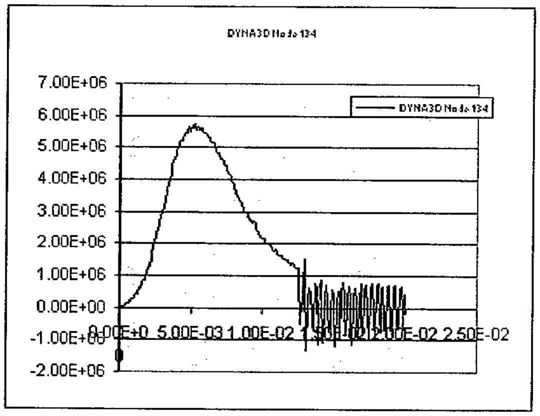

(a) Node 134

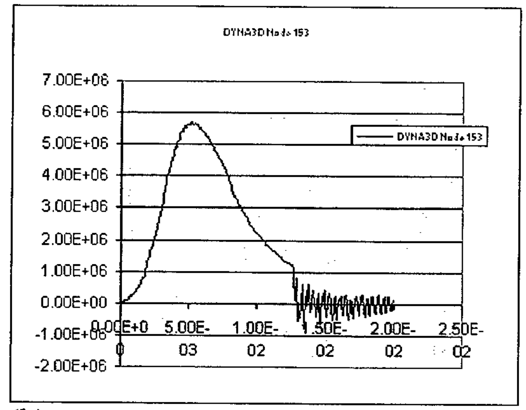

(b) Node 153

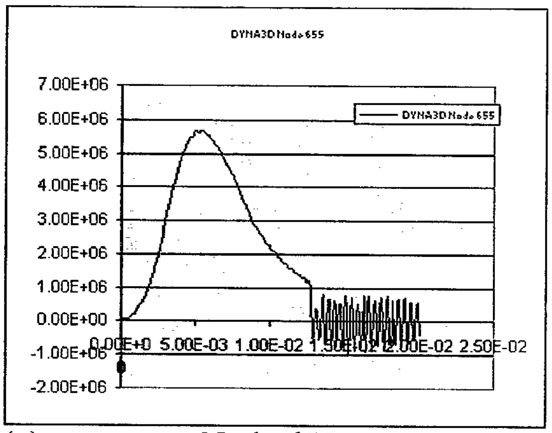

(c) Node 655

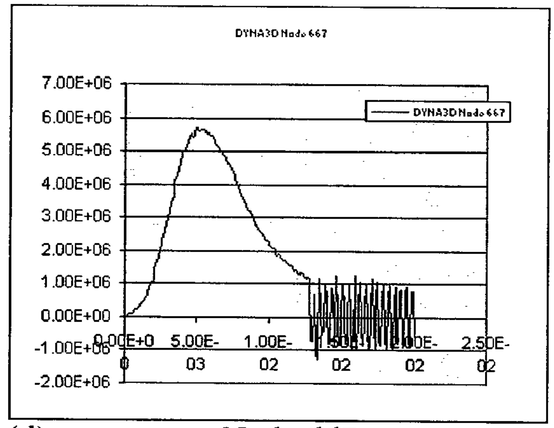

(d) Node 667

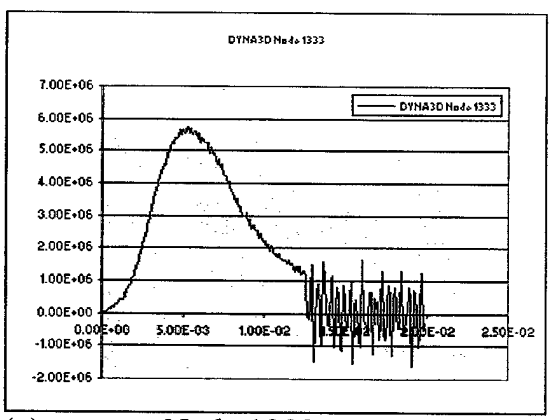

(e) Node 1333

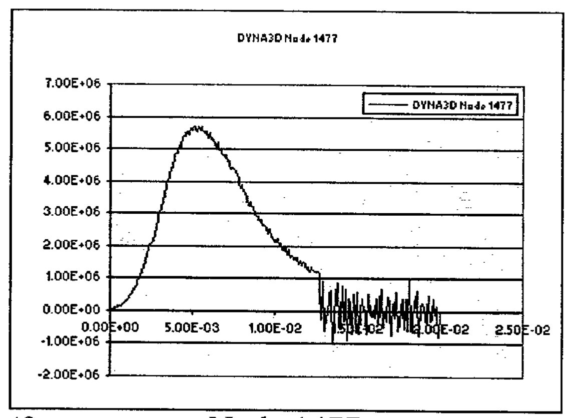

(f) Node 1477

Figure 8. Results From Cylinder Models.

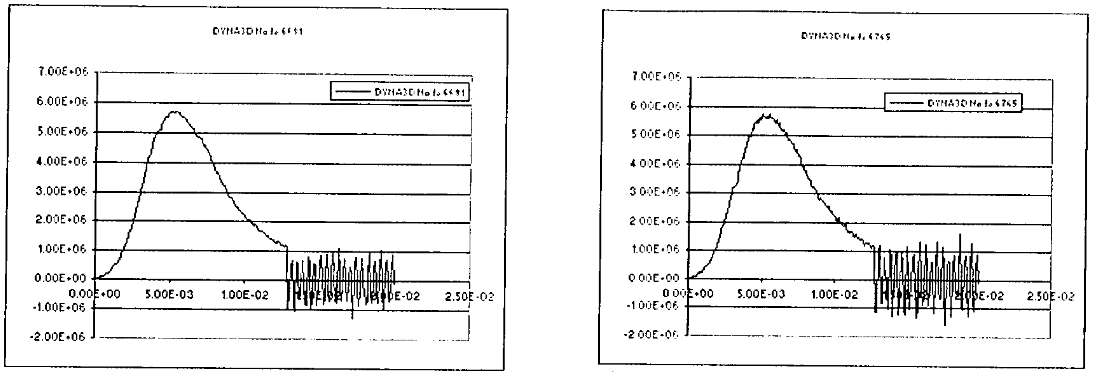

(g) Node 6681 (h) Node 6765

Figure 8. Results From Cylinder Models (continued).

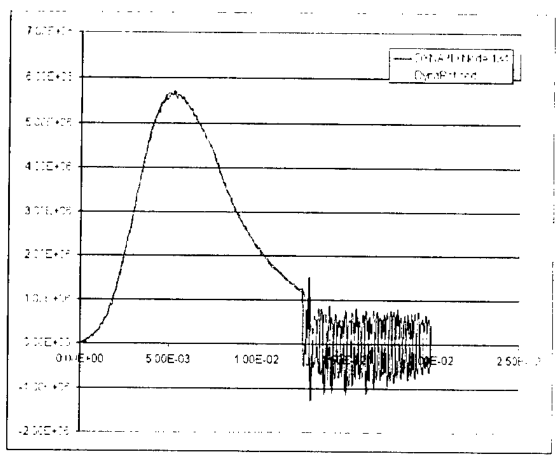

Figure 9. Comparison Between a Crude and Refined Model in DYNA3D.

between the crude and refined models is given in Figure 9. The temporal solution's convergence is assured in DYNA3D by the Courrant condition. However, in this plot, the importance of ensuring that the model has converged in the spatial regime is equally evident.

This discussion has shown that developing a model for the SADARM projectile cannot be limited to one single condition within the launch (i.e., peak pressure). Rather, the launching of a projectile with sophisticated components like SADARM requires the examination of various aspects of the launch, flight, and delivery of that system. Stress states at peak pressure, muzzle exit, peak spin rate, flight loads, and expulsion are just a few of the conditions that need to be examined. While components may survive the peak axial acceleration loads, they may be unable to survive the oscillatory nature of the exit loads or the off-axis spinning loads that are applied to the projectile during launch. Reducing all of these loading conditions may be difficult or impossible to do in a static analysis. Furthermore, possible gaps between components, impedance mismatching, and dynamic loads are not accounted for in a simple quasi-static analysis. Therefore, it is necessary to model as many of these troubling attributes prior to manufacturing and testing. Using more sophisticated transient techniques may enable the analyst to isolate potential failures and eliminate the design flaw prior to testing.

For example, DYNA3D offers a variety of material models, sliding interfaces, and a robust solver. Using DYNA3D, one can examine the full spectrum of loading conditions during the launch of a projectile.

4. Stack Model Details

A complete finite-element model of the SADARM projectile and gun system has been built to examine the launch and shot-exit transient loads on the projectile's major structural components. Additionally, this model can be used to examine the detailed analysis of individual components during launch as well. A brief review of the modeling attributes and assumptions are necessary to better understand and interpret the results.

The primary launch platform for the 155-mm SADARM projectile is the Paladin self-propelled artillery system and the M198 towed howitzer. Both gun tubes are nearly identical in length but have slight differences in chamber volume. However, differences in the recoil, mass, and platforms undoubtedly lead to difference in tube movement during launch, as well as projectile balloting.[1] Incorporating recoil and balloting loads is beyond the scope of the current effort and is therefore neglected. For this analysis, the M199 gun tube is modeled using

[1] Wilkerson, S. A., and R. P. Kaste. "An Improved Sabot Design and DYNA3D Analysis for the XM900E1 Kinetic Energy Projectile." BRL-TR-3359, U.S Army Ballistic Research Laboratory, Aberdeen Proving Ground, MD, June 1992.

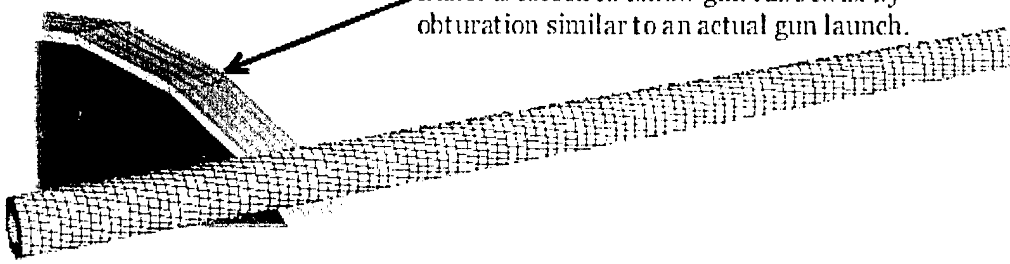

Figure 10. Gun-Tube Finite-Element Model and Gun-Projectile Interface.

eight-noded linear brick elements. Shown in Figure 10 is the finite element representation of the gun tube's launch section. A linear twist of 20 to 1 cal. is included in the model that is equivalent to the actual twist in the 155-mm system. The twist can be seen in the finite-element model in Figure 10.

The rear of the projectile is subjected to a pressure loading from the propellant. Using the IBHVG2 interior ballistics code, predictions are made regarding the launch of the SADARM projectile. Included are estimates of the pressure loading on the base of the projectile and the frictional force applied to the projectile at the obturator interface. The interface between the obturator shown in Figure 10 (gold color) and the tube (green color) was modeled in the finite-element model using DYNA3D's sliding-interface routines. Originally, it was thought that the frictional force could be included at this interface as a numerical algorithm coupling speed to frictional force. However, the implementation of this methodology resulted in excessive deformations in the obturation and gun tube. The result was that the bullet slipped between the twists and did not spin up correctly exiting the tube with only a percentage of the actual spin rate. On the other hand, if friction were not included, then the bullet exited at too high of a velocity and spin rate. Therefore, a traction force was added to the bullet's base at the approximate location of the obturation, equivalent to the force of the friction, as calculated by the IBHVG2 interior ballistics code. This prevented excessive deformation in the obturator, allowing the bullet to spin up at the proper rate, while balancing the pressure load with the actual frictional force so that the projectile exited the gun tube at the correct velocity and spin rate. Shown in

Figure 11 (a and b) is the pressure-time curve used for the 7R and 8S firing conditions in both metric and English systems. Figure 12 shows the base pressure and frictional force applied to the projectile.

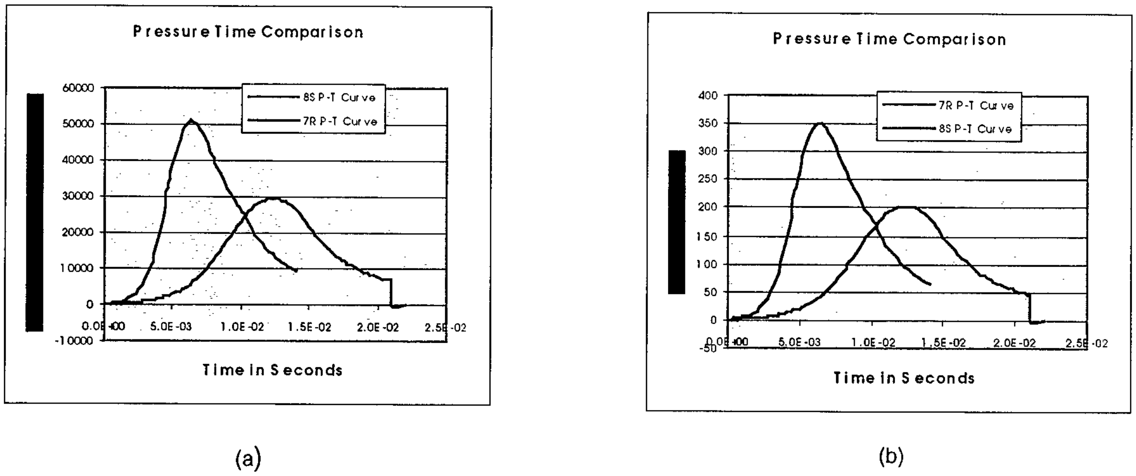

Figure 11. Pressure Time Curves Applied to the Base of the Projectile in the DYNA3D Finite-Element Model.

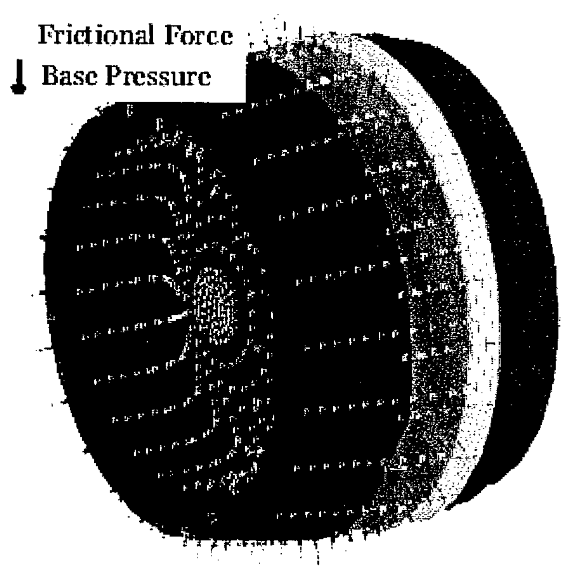

Figure 12. Base Pressure and Frictional Force Applied to the Projectile.

Both the 8S and 7R base loading conditions are considered. Inasmuch, the failures that have been observed have primarily been at higher load rates and in the aft submunition. The shell casing was also modeled using eight-noded brick elements. The base of the shell housing is rigidly attached to the base along the common interface. However, the shell casing is not rigidly attached to the base along the inner wall (Figure 13). If the entire interface were rigidly attached, this would have resulted in a model that was too stiff. Therefore, sliding interfaces were used, along the inner wall, preventing penetration while allowing gaps. Ultimately, this is a better representation of the actual one-and-a-half thread interface at that location than a rigid attachment would have been.

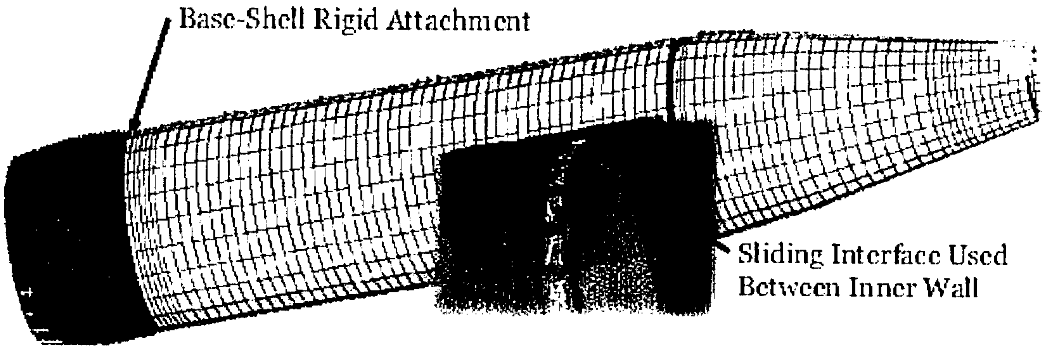

Figure 13. Base to Shell Attachment.

The fuse components were not modeled in detail. The fuse and expulsion charge-can and internal components were all broken down into lumped mass equivalents. Details in any of the models internal components can be added to examine one portion of the flight body at any time. However, this initial model is only being used to examine the load-carrying structural members. Figure 14 shows the finite-element model of the fuse parts.

The stack model consists of a number of components (Figure 15). As with the fuse, the stack model components were modeled using eight-noded brick elements. The model's primary use is to examine the load distribution and structural aspects of the internal SADARM stack assembly.

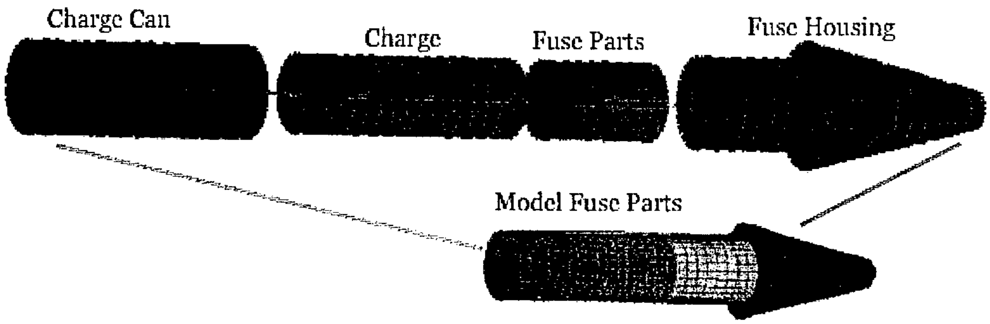

Figure 14. Finite-Element Model of Fuse Parts.

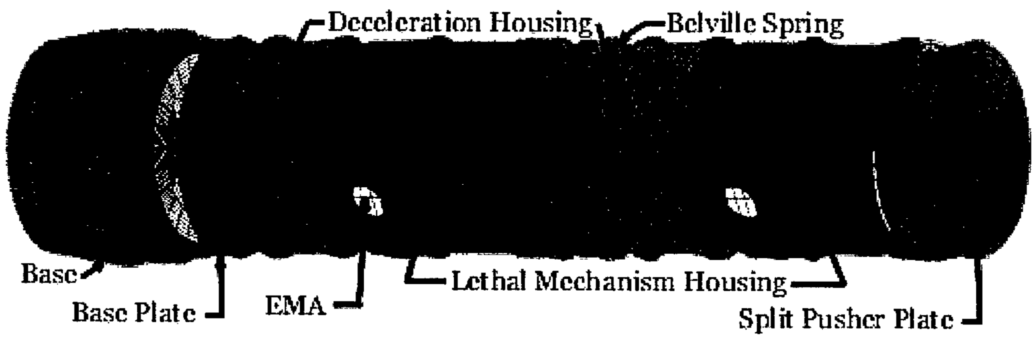

Figure 15. Finite-Element Model of SADARM's Stack Components.

Details can be added to any particular component to examine individual parts. This is discussed later in the report during the examination of the EMA. The parachute and other components inside of the deceleration housing are modeled as an equivalent lumped mass. The lethal mechanism, contains several components also modeled as equivalent lumped masses. Inside of the lethal mechanism, the EMA assembly and the Belleville spring are treated as lumped masses. The millimeter wave (MMW) assembly's components are also modeled using an equivalent mass. If all of the components making up the stack model were locked together rigidly,* the resulting stack model would become unrealistically stiff. To avoid this, sliding interfaces were used between parts. Figure 16 shows the sliding interfaces included between the

* When finite-element models are assembled, interfaces between associated parts need to be defined. One method of definition is called equivalency. Using this definition, nodes on one part are made coincident with the nodes from the other part. This forms a rigid attachment between the associated parts. Another method involves defining a mathematical relationship between the two parts. If nothing is done, then the parts can penetrate one another in an unrealistic manner.

associated components. Sliding interfaces allow gaps between associated parts eliminating tension while preventing interpenetration between parts under compression. This is an ideal interface for this application.

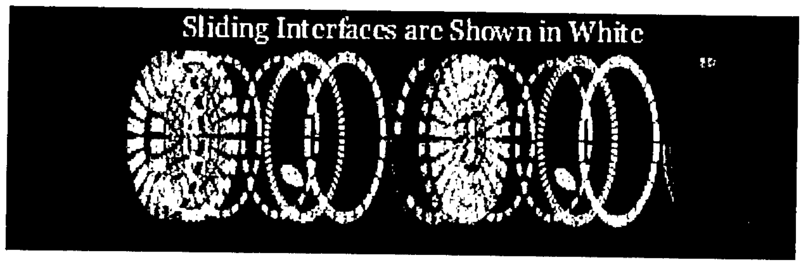

Figure 16. Sliding Interfaces Between Stack Components in the SADARM Finite-Element Model.

During the assembly of the SADARM stack model, the stack is dropped into the shell housing. Then a hydraulic press is used to compress the stack components and Bellville spring. A clamp is then applied to hold the assembly in place, while the base is screwed on leaving the stack in a state of compression. The approximate pressure is 2267.6 Ns, or 5000.0 lbs of force. To simulate this component in the model, the Bellville spring, two plates are connected in the middle and pressurized along their inner surfaces (see Figure 17). The inner faces have a sliding interface, which allows gaps between the spring's upper and lower surface, while preventing the surfaces from penetrating one another. Therefore, the model simulates the spring's function. Initially, a "no-gap" condition is assumed between the Bellville springs two surfaces. It is believed that there exists a gap between the plates, but the gap is not addressed in this model.

The primary purpose of this model was to examine the load-carrying portions of the SADARM projectile. The model provides an accurate method for simulating the transient launch environment of a 155-mm projectile. Furthermore, this model can be used as a flight vehicle to examine individual components. For example, a model of the EMA module has been built and will replace one or both of the lumped-mass EMA representations in this model. The resulting analysis will allow the examination of the combined structure, while eliminating many of the assumptions used in a quasi-static analysis. Figure 18 shows the cut-away view of the entire SADARM projectile.

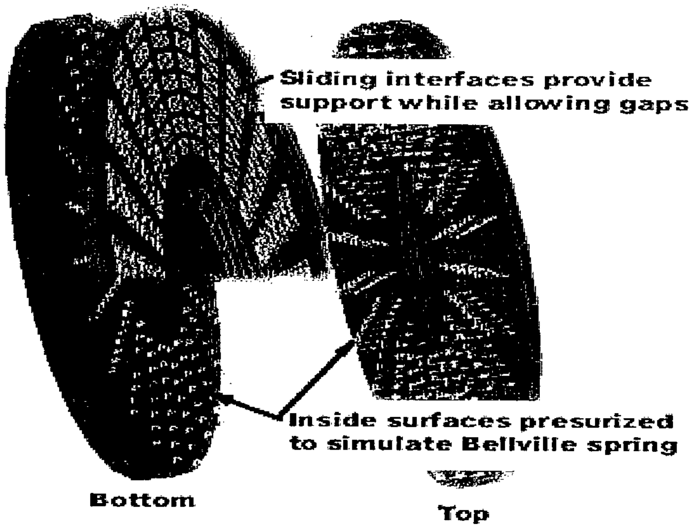

Figure 17. Bellville Spring Interface to Simulate Compressive Load on Stack Model.

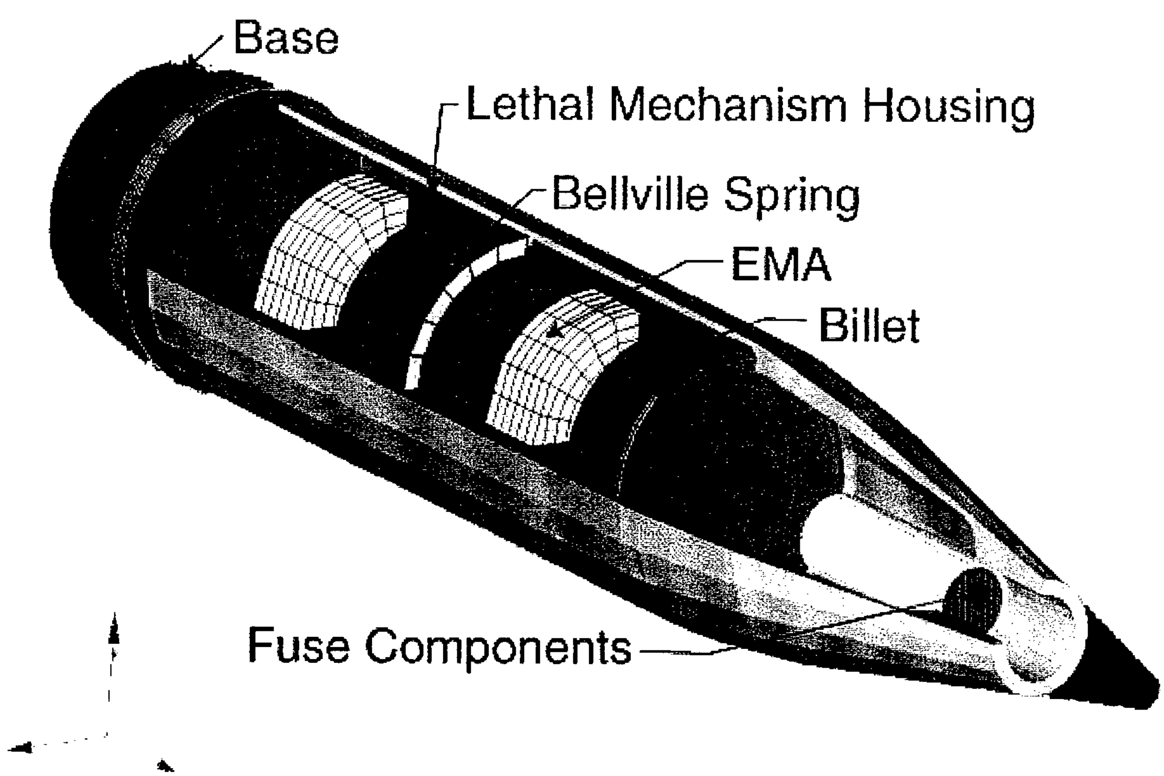

Figure 18. Cut-Away View of the SADARM Stack Model.

5. Results

The stack model developed for this analysis is the most complicated and accurate model developed for the SADARM program. The model has approximately 70,000 eight-noded brick elements, more than a dozen sliding interfaces, and numerous other boundary conditions. Validating such a model is a time-consuming process that requires advanced visualization techniques and experience. Small mistakes allow the model to execute, while potentially giving incorrect results at a particular location within the model's structure. However, if the boundary conditions are applied correctly, the structure must follow the basic laws of nature. Therefore, the accelerations, velocities, and displacements must match the internal ballistics solutions where $F = ma$. That is, the pressure loading on the base of the projectile will accelerate the mass at a predetermined rate. The internal ballistics solutions used to generate the pressure time curves are given in Figure 11. The internal ballistics code also calculates the acceleration, velocity and displacement of the projectile. These predictions have been shown to be accurate. Therefore, a comparison with the internal ballistics code's prediction is a good first check of the result's overall accuracy. Figure 19 (a) compares the displacement estimates for the projectile form IBHVG2 with the DYAN3D calculations. Similarly, Figure 19 (b) compares the velocity estimates for the two calculations. As can be seen in Figure 19, the results are reasonably close. This is a good indication that the projectile is being accelerated at the proper rate and that the stresses and strains will be accurately reflected in the model. Another parameter that needs to be checked is the spin rate. If the correct spin rate is being imparted to the projectile, the projectile should rotate two times during its in-bore flight. By tracking a node near the surface of the projectile's housing, one can determine how many revolutions the projectile has made during its in-bore flight (see Figure 20).

A comparison between the 7R and 8S loading conditions is made. As seen in Figures 21–24, the 8S loading condition pushes many of the structural components close to the limit of their design. In these results, von-Mises equivalent stress is used for comparison. The design philosophy is to keep all of the stress in the structure below yield. The original shell casing used

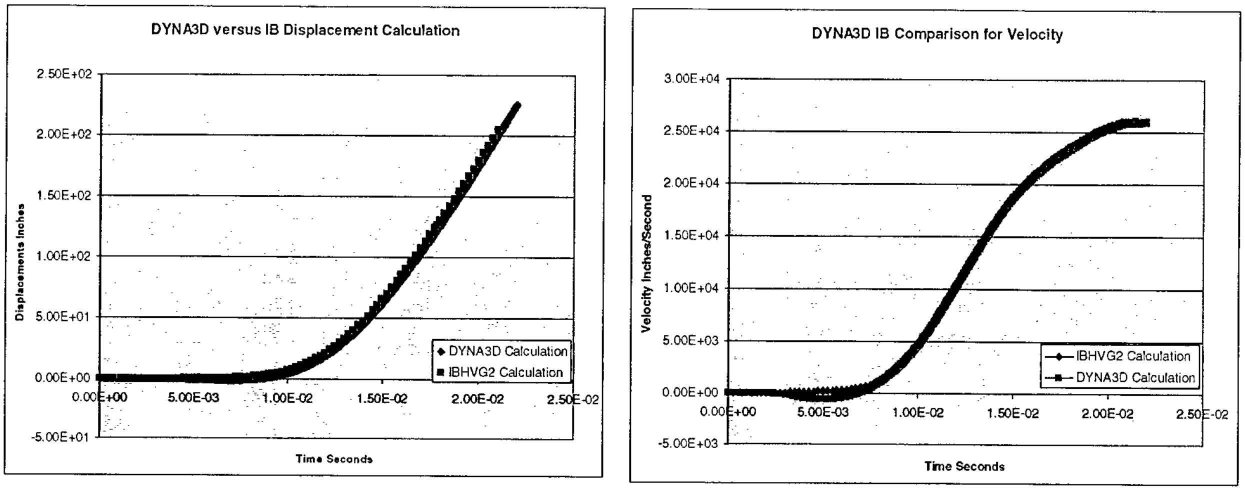

(a) (b)

Figure 19. Displacement and Velocity Comparisons Between the IBHVG2 Code and DYNA3D's Finite-Element Calculations.

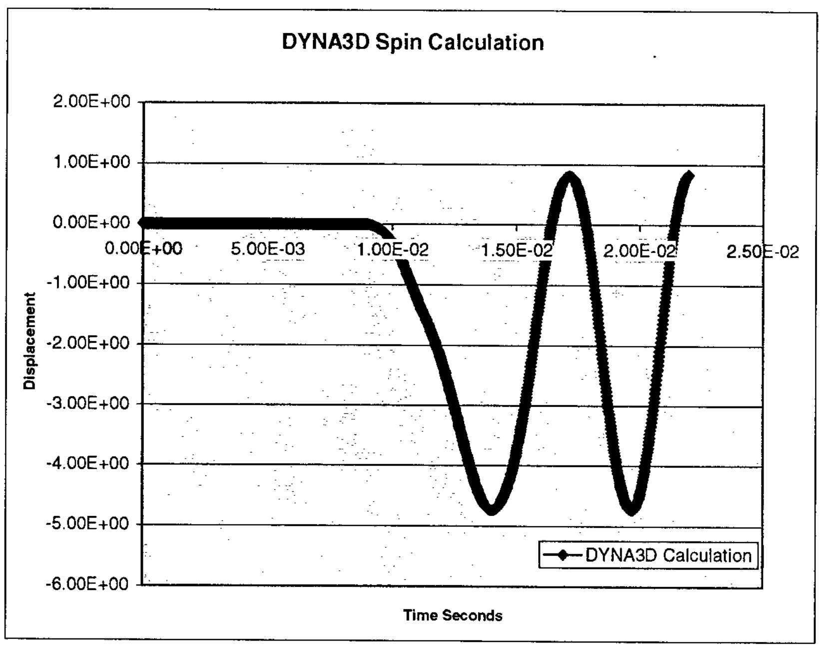

Figure 20. Checking the Projectile's Number of Revolutions While In-Bore.

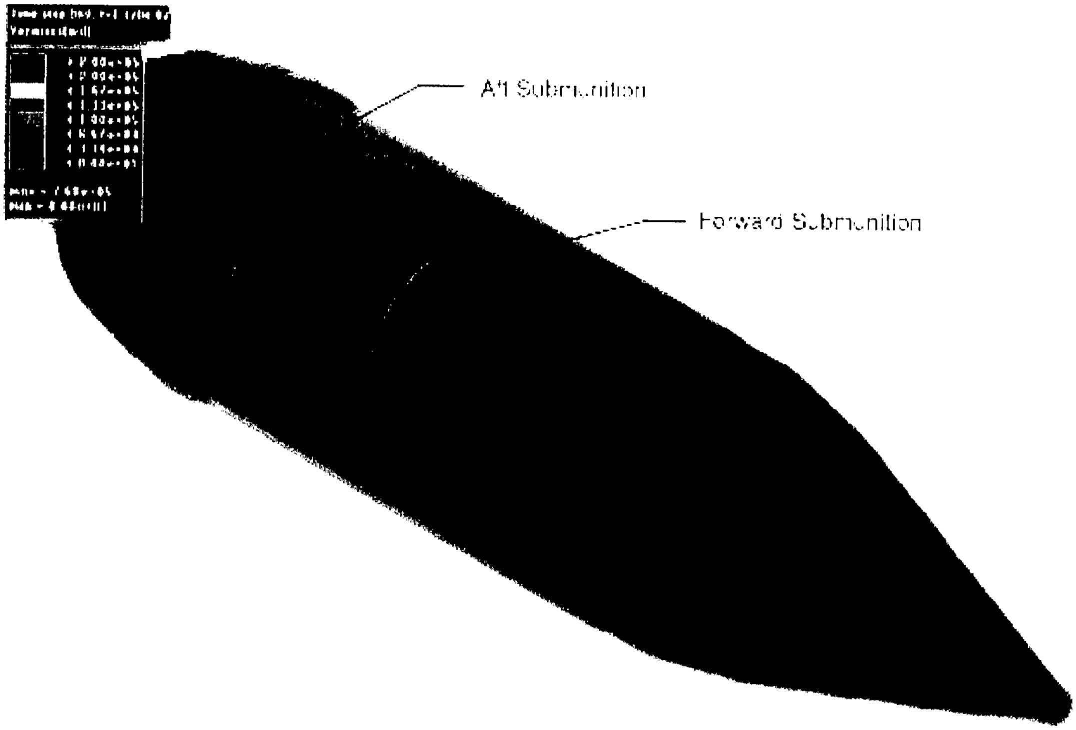

Figure 21. Von-Mises Stress Contours at Peak Pressure for a 7R Firing.

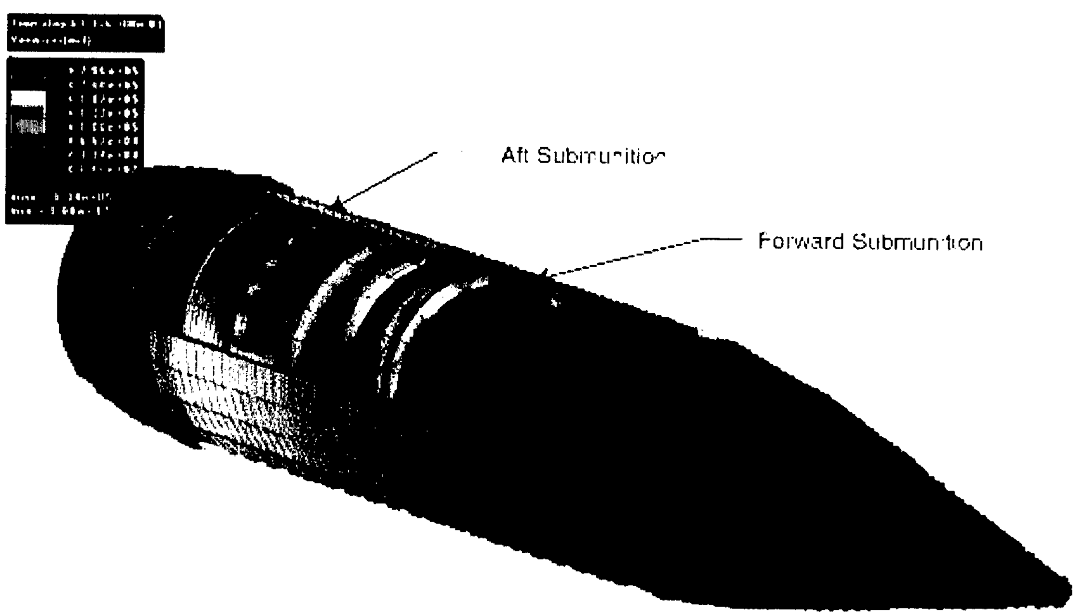

Figure 22. Von-Mises Stress Contours at Peak Pressure for an 8S Firing.

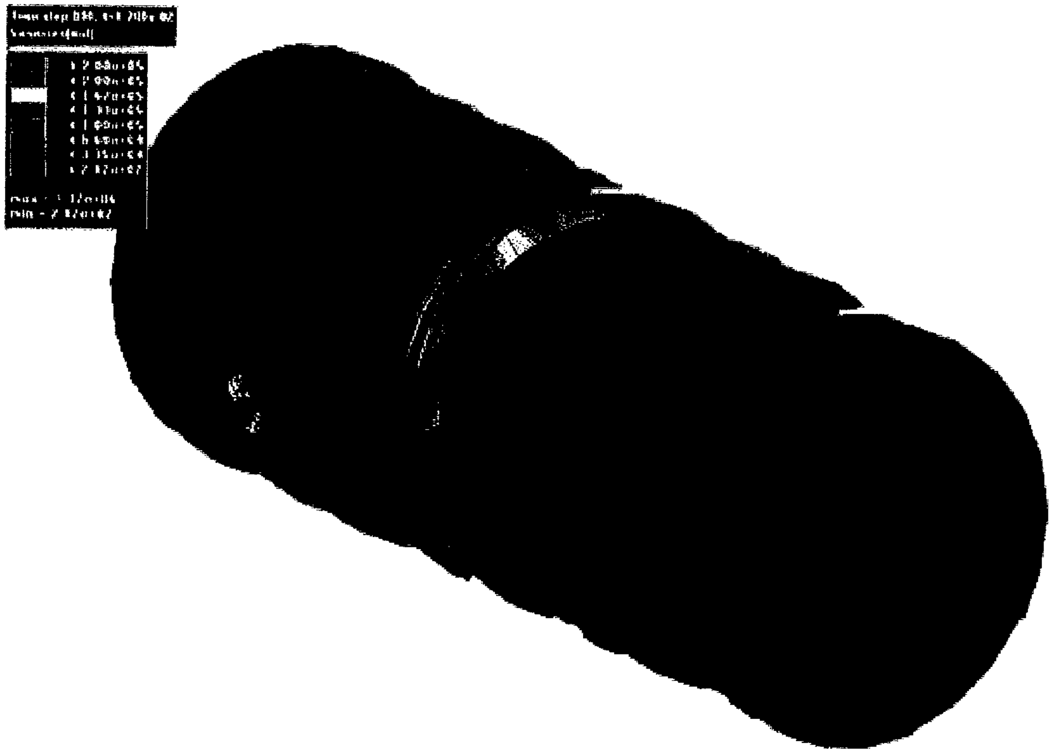

Figure 23. Von-Mises Stress Contours at Peak Pressure for a 7R Firing.

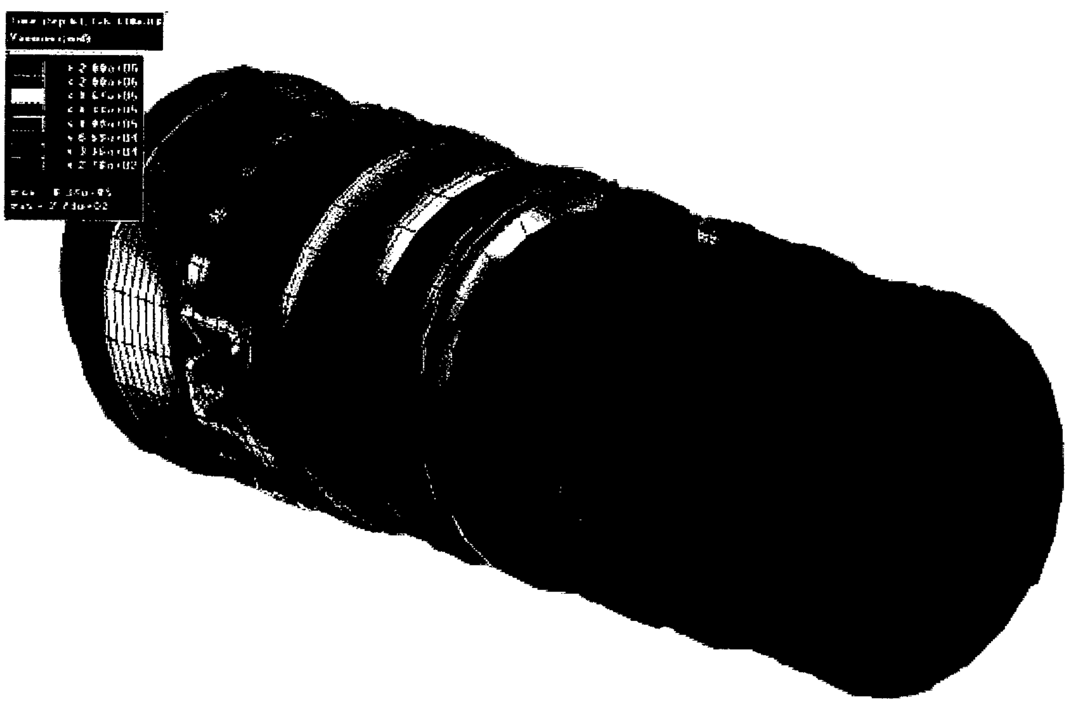

Figure 24. Von-Mises Stress Contours at Peak Pressure for an 8S Firing.

for SADARM was manufactured from 4340 steel, with an approximate yield strength of 195 kpsi. Subsequently, the steel choice for the shell casing was changed to a titanium-based Maraging-steel, which increased its yield to approximately 250 kpsi after the final heat treatment. For this analysis, the maximum von-Mises stress level was set to red for stresses above 200 kpsi and pink for levels within 20 kpsi of the limit. Figures 21 and 22 show the von-Mises stress contours for the 7R and 8S firing conditions at peak pressure in a cut-away view of the complete SADARM stack model. As can be seen in these figures, the aft submunition is experiencing higher stress levels than the forward submunition. It is not surprising to note that the aft submunition also experiences a higher failure rate. Figures 23 and 24 show a cut-away view of the internal stack components. Higher stress levels can also be seen near knockout holes in the aft lethal mechanism housing and near the intermediate frequency electronics (IFE) ring recess areas.

All of the contours provided were at peak pressure. For the stack's structural load-carrying components, this is a limiting condition. Although the spin rate offers no real concerns for the lethal mechanism housing and shell casing, the spin load is of concern for the electronic chips and other hardware found in the EMA housing. Additionally, at shot exit, the base pressure drops off very rapidly inducing stress waves in the structure. This phenomenon can be clearly seen in the examples given in Figure 8. To help analyze the huge amount of data generated from a transient analysis, movies are made to reduce the data into a palatable form. Movies of the entire structure are analyzed, as well as subcomponents and individual components. The results are then reanalyzed at specific points* in the launch to identify component weaknesses. Parts can then be redesigned to strengthen and reduce their design margin.

6. Conclusions

Finite-element methods have proven their worth in analyzing complex structures under varying load conditions. Using finite-element methods, a completed structure can be examined

* This was done here as well. The results presented here are for the stack model at peak pressure. One of the advantages of a transient analysis is that it examines all of the loads throughout the launch cycle. Then, using multimedia technology, one can analyze the data and focus on the important aspects of the problem rapidly.

in detail to expose weakness in the design. For a number of years, finite-element methods have been employed to examine the launch of projectiles from gun system with success. Typical analysis examined the peak-pressure loading condition in-bore using a quasi-static balance of pressure and acceleration loading. The results proved useful in designing a projectile structure capable of surviving gun launch. The initial design of the SADARM projectile employed these basic techniques. However, when failures that were not predicted in the analysis began to turn up, a closer look was necessary.

Transient analysis offered the opportunity to look at the spectrum of loading conditions that the projectile was being exposed to. The importance of a transient analysis was also examined using simple models. Based on results from these simple models at shot exit and the closeness of the peak stresses to yield, an argument for the use of DYNA3D seems evident. The DYNA3D code offered a number of advantages for the analysis of gun-launched projectiles, as demonstrated here. One of the most important is the sliding-interface corrections available in the DYNA3D code which allow gaps while preventing inner penetration. These interfaces allow the projectile and gun system to be modeled together and the entire launch cycle to be accounted for. The resulting analysis contains many of the loads not considered in a static finite-element method approximation, including balloting and transient stress waves during launch and shot exit.

The analysis presented here represents an improvement over conventional finite-element method static analysis techniques previously used to analyze gun-launched projectiles. The analysis eliminates many of the troubling boundary conditions and assumptions required by a quasi-static analysis. The resulting model is the most accurate and reliable to date. The resulting predictions can be used with a high degree of confidence to improve and optimize current and future smart munitions like SADARM.

INTENTIONALLY LEFT BLANK.

NO. OF COPIES	ORGANIZATION
2	DEFENSE TECHNICAL INFORMATION CENTER DTIC DDA 8725 JOHN J KINGMAN RD STE 0944 FT BELVOIR VA 22060-6218
1	HQDA DAMO FDT 400 ARMY PENTAGON WASHINGTON DC 20310-0460
1	OSD OUSD(A&T)/ODDDR&E(R) R J TREW THE PENTAGON WASHINGTON DC 20301-7100
1	DPTY CG FOR RDA US ARMY MATERIEL CMD AMCRDA 5001 EISENHOWER AVE ALEXANDRIA VA 22333-0001
1	INST FOR ADVNCD TCHNLGY THE UNIV OF TEXAS AT AUSTIN PO BOX 202797 AUSTIN TX 78720-2797
1	DARPA B KASPAR 3701 N FAIRFAX DR ARLINGTON VA 22203-1714
1	US MILITARY ACADEMY MATH SCI CTR OF EXCELLENCE MADN MATH MAJ HUBER THAYER HALL WEST POINT NY 10996-1786

NO. OF COPIES	ORGANIZATION
1	DIRECTOR US ARMY RESEARCH LAB AMSRL D D R SMITH 2800 POWDER MILL RD ADELPHI MD 20783-1197
1	DIRECTOR US ARMY RESEARCH LAB AMSRL DD 2800 POWDER MILL RD ADELPHI MD 20783-1197
1	DIRECTOR US ARMY RESEARCH LAB AMSRL CI AI R (RECORDS MGMT) 2800 POWDER MILL RD ADELPHI MD 20783-1145
3	DIRECTOR US ARMY RESEARCH LAB AMSRL CI LL 2800 POWDER MILL RD ADELPHI MD 20783-1145
1	DIRECTOR US ARMY RESEARCH LAB AMSRL CI AP 2800 POWDER MILL RD ADELPHI MD 20783-1197
	ABERDEEN PROVING GROUND
4	DIR USARL AMSRL CI LP (BLDG 305)

INTENTIONALLY LEFT BLANK.

REPORT DOCUMENTATION PAGE

Form Approved
OMB No. 0704-0188

1. AGENCY USE ONLY *(Leave blank)*	2. REPORT DATE	3. REPORT TYPE AND DATES COVERED
	September 2000	Final, January 1999 - September 2000

4. TITLE AND SUBTITLE
Developing a Transient Finite Element Model to Simulate the Launch Environment of the 155-mm SADARM Projectile

5. FUNDING NUMBERS
1L162618AH80

6. AUTHOR(S)
Stephen Wilkerson, David Hopkins, George Gazonas, and Morris Berman

7. PERFORMING ORGANIZATION NAME(S) AND ADDRESS(ES)
U.S. Army Research Laboratory
ATTN: AMSRL-WM-BC
Aberdeen Proving Ground, MD 21005-5066

8. PERFORMING ORGANIZATION REPORT NUMBER
ARL-TR-2341

9. SPONSORING/MONITORING AGENCY NAMES(S) AND ADDRESS(ES)

10. SPONSORING/MONITORING AGENCY REPORT NUMBER

11. SUPPLEMENTARY NOTES

12a. DISTRIBUTION/AVAILABILITY STATEMENT
Approved for public release; distribution is unlimited.

12b. DISTRIBUTION CODE

13. ABSTRACT *(Maximum 200 words)*
Projectiles like SADARM, with delicate electronic components, need robust designs that are able to survive high "g" accelerations and spin rates. Unfortunately, the packaging of these components and their space requirements reduce the design's safety margin. Therefore, considerable care must be used in analyzing the structural package. Conventional projectiles are typically analyzed using a quasi-static, axisymmetric, finite-element approach that balances the peak propellant pressure on the base of the projectile with an equivalent acceleration. In most circumstances, the robustness of the design makes this approach more than sufficient for identifying problem areas in the structure. However, the internal components used in SADARM are sensitive to off-axis loading such as that caused by spin rate or the rapid unloading of the projectile's base that occurs at muzzle exit. Additionally, stress waves caused by balloting and impedance mismatching within the stack design only serve to further reduce the design margin. To compensate for the reduced design margin and the increased source of potentially damaging loads, more sophisticated finite-element techniques need to be employed. The techniques presented here represent a modern approach to analyzing the projectile's launch loading conditions over traditional techniques.

14. SUBJECT TERMS
DYNA3D solution, transient finite element analysis

15. NUMBER OF PAGES
32

16. PRICE CODE

17. SECURITY CLASSIFICATION OF REPORT	18. SECURITY CLASSIFICATION OF THIS PAGE	19. SECURITY CLASSIFICATION OF ABSTRACT	20. LIMITATION OF ABSTRACT
UNCLASSIFIED	UNCLASSIFIED	UNCLASSIFIED	UL

NSN 7540-01-280-5500

Standard Form 298 (Rev. 2-89)
Prescribed by ANSI Std. 239-18 298-102

INTENTIONALLY LEFT BLANK.

USER EVALUATION SHEET/CHANGE OF ADDRESS

This Laboratory undertakes a continuing effort to improve the quality of the reports it publishes. Your comments/answers to the items/questions below will aid us in our efforts.

1. ARL Report Number/Author ARL-TR-2341 (Wilkerson) Date of Report September 2000

2. Date Report Received ______

3. Does this report satisfy a need? (Comment on purpose, related project, or other area of interest for which the report will be used.) ______

4. Specifically, how is the report being used? (Information source, design data, procedure, source of ideas, etc.) ______

5. Has the information in this report led to any quantitative savings as far as man-hours or dollars saved, operating costs avoided, or efficiencies achieved, etc? If so, please elaborate. ______

6. General Comments. What do you think should be changed to improve future reports? (Indicate changes to organization, technical content, format, etc.) ______

CURRENT ADDRESS

Organization

Name E-mail Name

Street or P.O. Box No.

City, State, Zip Code

7. If indicating a Change of Address or Address Correction, please provide the Current or Correct address above and the Old or Incorrect address below.

OLD ADDRESS

Organization

Name

Street or P.O. Box No.

City, State, Zip Code

(Remove this sheet, fold as indicated, tape closed, and mail.)

(DO NOT STAPLE)

DEPARTMENT OF THE ARMY

OFFICIAL BUSINESS

NO POSTAGE
NECESSARY
IF MAILED
IN THE
UNITED STATES

BUSINESS REPLY MAIL
FIRST CLASS PERMIT NO 0001,APG,MD

POSTAGE WILL BE PAID BY ADDRESSEE

DIRECTOR
US ARMY RESEARCH LABORATORY
ATTN AMSRL WM BC
ABERDEEN PROVING GROUND MD 21005-5066